Journal of Alloys and Compounds 628 (2015) 230–235

Contents lists available at ScienceDirect

Journal of Alloys and Compounds

journal homepage: www.elsevier.com/locate/jalcom

# Giant magnetoresistance and field-induced magnetic phase transitions in $Gd_7Rh_3$ studied on single crystals

Takanori Tsutaoka [a,*], Takuya Matsushita [a], Alexey V. Proshkin [b,c], Evgeny G. Gerasimov [b], Pavel B. Terentev [b], Nikolai V. Baranov [b,c]

[a] Graduate School of Education, Hiroshima University, Higashi-Hiroshima 739-8524, Japan
[b] Institute of Metal Physics, Ural Branch of RAS, 620990 Ekaterinburg, Russia
[c] Institute of Natural Sciences, Ural Federal University, 620083 Ekaterinburg, Russia

ARTICLE INFO

*Article history:*
Received 16 November 2014
Received in revised form 16 December 2014
Accepted 17 December 2014
Available online 31 December 2014

*Keywords:*
$Gd_7Rh_3$
Magnetization
Magnetoresistance
Field-induced magnetic transition
Magnetic phase diagram

ABSTRACT

Magnetization measurements in steady and pulsed fields and magnetoresistance measurements in different field-current geometries on single crystalline samples have been employed to study the field-induced magnetic phase transitions in the antiferromagnetically (AF) ordered compound $Gd_7Rh_3$ with hexagonal crystal structure of the $Th_7Fe_3$ type. Below $T_N$ = 141 K, the magnetic structure transformations from AF to the forced ferromagnetic (FF) state, which are accompanied by a giant reduction of the electrical resistivity (up to 7 times at low temperatures), were observed under the magnetic fields along the *c*-axis and in the basal plane. This giant magnetoresistance is associated with magnetic superzone effects. The negative temperature coefficient of the electrical resistivity and a large magnetoresistance were also observed in the paramagnetic region in $Gd_7Rh_3$; which are suggested to result from the retention of short-range AF correlations in a wide temperature range above $T_N$.



## 1. Introduction

Intermetallic compound $Gd_7Rh_3$ crystallizes in the $Th_7Fe_3$-type hexagonal structure with the space group $P6_3mc$ [1,2]. In this structure, $Gd^{3+}$ ions occupy three non-equivalent crystallographic sites. Studies of magnetic and electrical properties of $Gd_7Rh_3$ performed on polycrystalline samples as well as on single crystals have revealed that $Gd_7Rh_3$ possesses antiferromagnetic (AF) state below $T_N$ = 141 K and exhibits field-induced magnetic phase transitions along the *c*-axis and in the *c*-plane [3,4]. Since it is difficult to carry out the neutron diffraction measurements on the Gd compounds due to the large neutron absorption, the magnetic structure of $Gd_7Rh_3$ and its change at the field-induced phase transitions has not been examined. However, from the magnetization measurements performed along the main crystallographic directions on a single crystalline sample, the Gd magnetic moments in $Gd_7Rh_3$ are suggested to be aligned in the *c*-plane of the hexagonal crystal lattice [5].

It has also been found that $Gd_7Rh_3$ exhibits several features in the behavior of the electrical resistivity with temperature and in an applied magnetic field: (a) almost zero or negative temperature coefficient ($d\rho/dT$) in a wide temperature range above magnetic ordering temperature; (b) the resistivity hump just below $T_N$ indicating the superzone gap formation due to an antiferromagnetic structure; (c) the metallic-type resistivity change at low temperatures; and (d) a large magnetoresistance observed not only in the AF ordered state but even in the paramagnetic region up to near the room temperature [6–8]. Similar peculiarities in electrical properties have also been reported for some other $R_7Rh_3$ compounds such as $Sm_7Rh_3$ [9], $Ho_7Rh_3$ [10] and $Er_7Rh_3$ [11]; the giant magnetoresistance (GMR) has been revealed in $Tb_7Rh_3$ [12] and $Dy_7Rh_3$ [13]. For the antiferromagnetic compound $Tb_7Rh_3$ ($T_N$ = 91 K), the magnetization curves of a non-Brillouin shape were observed well above $T_N$. Such an unusual behavior of the magnetization in paramagnetic region was considered as an indication on the presence of regions with the short-range antiferromagnetic order within paramagnetic matrix [14]. As was suggested in [14], such short-range antiferromagnetic correlations may result in the presence of an additional magnetic contribution to the electrical resistivity at temperatures above $T_N$. This property has been observed in the isostructural $Nd_7Pd_3$, too [15].

In this study, we have carried out the magnetization measurements on $Gd_7Rh_3$ single crystals in magnetic fields applied along main crystallographic directions and the magnetoresistance measurements in different field-current geometries aiming to reveal

* Corresponding author.
*E-mail address:* tsutaok@hiroshima-u.ac.jp (T. Tsutaoka).

http://dx.doi.org/10.1016/j.jallcom.2014.12.167
0925-8388/

the magnetic phase transitions and to construct the magnetic field $H$ – temperature $T$ phase diagram along the $c$- and $b$-axes. Bearing in mind the pervious data [4] indicating a pronounced deviation of the paramagnetic susceptibility of $Gd_7Rh_3$ from the Curie–Weiss behavior in the temperature range from $T_N$ up to 470 K, together with the magnetization and magnetoresistance measurements in steady magnetic fields up to 120 kOe, we used pulsed-field magnetization measurements up to 350 kOe in order to clarify the magnetic state of this compound above the magnetic ordering temperature.

## 2. Experimental

The polycrystalline ingots of $Gd_7Rh_3$ were prepared by arc-melting the constituent elements of 99.9% Gd and 99.96% Rh in high purity argon atmosphere. In this process, the ingots were turned over and remelted several times to ensure homogeneity. Single crystals were grown by the Czochralski method from single-phase polycrystalline samples using a tri-arc furnace. Rectangular samples were cut from the ingots. All samples were annealed at 300 °C for 30 h in an evacuated quartz tube. Powder X-ray diffraction indicated that the all samples were in single phase with the $Th_7Fe_3$-type hexagonal structure. The crystal orientation was determined by the back reflection Laue method. We define the $b$-axis as the [1 2 0] direction, which is perpendicular to the $a$-axis in the $c$-plane.

The magnetization $M$ was measured in pulsed fields up to 350 kOe by an induction method with a set of compensated pickup coils in the temperature range from 4 K to 280 K. Magnetoresistance $\Delta\rho/\rho$ was measured by the ac four-terminal method in magnetic fields up to 120 kOe at several temperatures up to 220 K. Temperature variation of the electrical resistivity $\rho$ was also measured by using a dc four-terminal method in the temperature range from 4.2 K to 300 K.

## 3. Results and discussion

Bearing in mind that the electrical resistivity in AF ordered compounds with metallic conductivity closely relates to arrangement of magnetic moments we plotted in Fig. 1 the magnetization curves measured along the principal crystallographic directions of $Gd_7Rh_3$ together with field dependences of the magnetoresistance. These $M$ ($H$) curves were taken from our previous work [5]. As follows from Fig. 1(a), the $c$-axis magnetization $M$ linearly increases with magnetic field $H$ up to about 35 kOe; a single magnetic phase transition takes place at $H_{Cc}$ = 73.2 kOe and the saturation is observed at about 80 kOe. Saturation magnetization indicates 7.0 $\mu_B$/Gd; this coincides with the $gJ$ value of $Gd^{3+}$ ion. The $M$–$H$ curve along the $b$-axis shows two successive phase transitions: the first spin-flop like transition at $H_{Cb1}$ = 59.5 kOe and the second transition to the forced ferromagnetic (FF) state $H_{Cb2}$ = 79.9 kOe, respectively; magnetization value at 120 kOe is 6.6 $\mu_B$/Gd, which is smaller than that along the $c$-axis [5]. However, the magnetization measurements up to 350 kOe have shown that magnetization gradually increases with magnetic field above 120 kOe and almost saturates at 350 kOe indicating the value of 7.0 $\mu_B$/Gd. These data are indicative of the parallel alignment of Gd magnetic moments in the forced ferromagnetic (FF) states realized in both the $c$-direction and the $c$-plane.

The magnetoresistance ($\Delta\rho/\rho$ vs. $H$) curves for $Gd_7Rh_3$ measured at 4 K are shown in Fig. 1(b) when the external magnetic field applied along the $b$- and $c$-axes and the electric current $j$ directed along the $c$-axis. The $\Delta\rho/\rho$ value at the $H$ // $j$ // $c$ geometry is almost constant up to 40 kOe and shows a giant decrease with further increasing field up to a critical value $H_{Cc}$ corresponding to the AF–FF transition. On the other hand, the $\Delta\rho/\rho$ initially increases with increasing $H$ applied along the $b$-axis ($H$ // $b$ and $j$ // $c$ geometry) and demonstrates two successive drops corresponding to the magnetic phase transitions at $H_{Cb1}$ and $H_{Cb2}$. Since the inflection points of the $\Delta\rho/\rho$–$H$ curves coincide with the critical fields $H_{Cb1}$ and $H_{Cb2}$, as shown in the inset of Fig. 1(b), the critical fields of the magnetic transitions can be determined from the magnetoresistance curves as well as the magnetization ones. A small

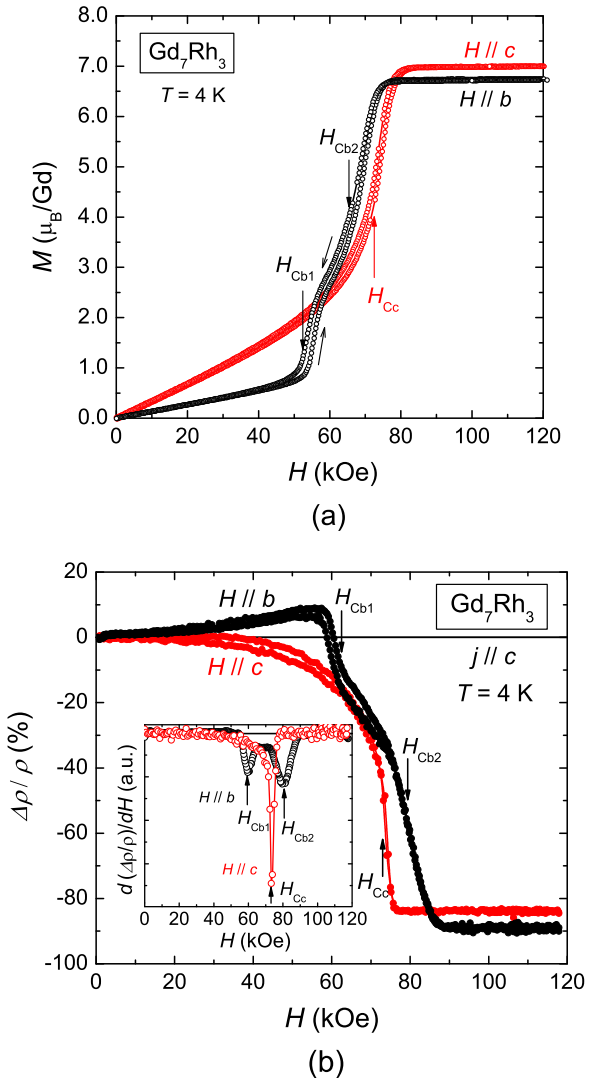


**Fig. 1.** Magnetization curves (a) and the magnetoresistance $\Delta\rho/\rho$ as a function of the external magnetic field $H$ (b) along the $b$- and $c$-axes at 4.0 K for $Gd_7Rh_3$ single crystal. The inset in (b) shows the $d(\Delta\rho/\rho)/dH$ vs. $H$ curves.

hysteresis is observed on both the magnetization and magnetoresistance curves around critical fields, which implies the first order character of the transitions.

The $\Delta\rho/\rho$ value at 100 kOe reaches −84% and −89% when the field applied along the $c$- and $b$-axis, respectively. The fairly low difference between these $\Delta\rho/\rho$ values indicates that the orientation of the magnetization has a little influence on the resistivity of $Gd_7Rh_3$ in the FF state. As can be seen in many other antiferromagnets, a giant reduction of the resistivity under the external magnetic field in $Gd_7Rh_3$ is apparently originated by the disappearance of the superzones and energy gaps on the superzone boundaries at AF–FF transition. As shown by Elliot and Wedgwood [16], the superzone formation results in the resistivity increase in antiferromagnets. Since the first-order type phase transitions occur through the appearance of the nuclei of a new field-induced phase and the growth of the volume of nuclei via domain (interphase) wall motion, a positive magnetoresistance observed in $Gd_7Rh$ with increasing $H$ along the $b$-axis up to a critical value may be attributed to the scattering of $s$ electrons by the magnetic moments distributed in the interphase boundaries as the magnetic defects and to the reflections of a part of the conduction electrons from a potential barrier at the interphase boundary caused by the different energy

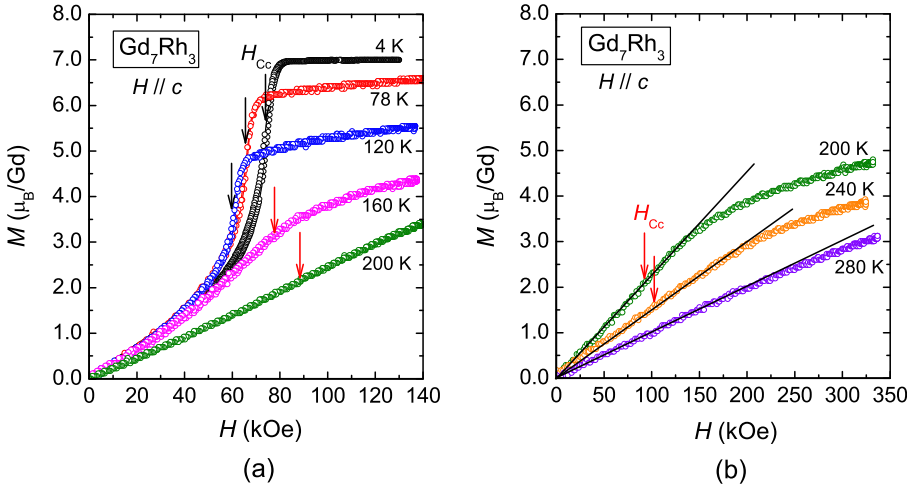


**Fig. 2.** Magnetization curves along the *c*-axis for a $Gd_7Rh_3$ single crystal at various temperatures.

spectra of conduction electrons in the phases with different magnetic structures [17]. Unlike the $H$ // $b$ case, when the field is applied along the *c*-axis, the gradual rotation of Gd moments from the *c*-plane to the *c*-axis with increasing $H$ up to $H_{Cc}$ leads to the monotonous reduction of the resistivity.

The magnetization curves of $Gd_7Rh_3$ measured along the *c*-axis at several temperatures from 4 to 280 K are shown in Fig. 2. As indicated in Fig. 2(a), the critical field $H_{Cc}$ along the *c*-axis decreases with increasing temperature in the antiferromagnetic state below 141 K. We noticed that above $T_N$, i.e. in the paramagnetic state, the $M$–$H$ curves exhibit a non-Brillouin shape with an inflection point up to about 240 K. The critical field corresponding to the inflection point increases with increasing temperature as shown by arrows in Fig. 2(b). This result indicates that in $Gd_7Rh_3$, the antiferromagnetic regions (clusters) with short ranged correlations may persist above $T_N$ up to relatively high temperatures and the inflection point on the $M$–$H$ curves may be associated with the field-induced transition in such antiferromagnetic clusters. This type of magnetization behavior was observed in the isostructural compound $Tb_7Rh_3$ [14] and in $R_3T$-type compounds ($R$ = Gd, Tb; $T$ = Ni, Co) [18], too. For $Tb_3Ni$ and $Tb_3Co$, the persistence of short-range magnetic order up to the temperatures greater than 5–6 times of the Neel temperature was evidenced by powder neutron diffraction measurements [18].

Fig. 3 shows the longitudinal magnetoresistance curves along the *c*-axis ($j$ // $c$ and $H$ // $c$) at various temperatures. In Fig. 3(a), the curves are plotted with offset in order to make clear the temperature evolution. In the magnetically ordered state, the critical field $H_{Cc}$ gradually decreases with increasing temperature and disappears at $T_N$. Simultaneously, $\Delta\rho/\rho$ reduces and shows a value of about −28% at $H$ = 100 kOe and $T$ = 140 K. As can be seen in Fig. 3(b), the magnetoresistance curve above $T_N$ also exhibits the inflection point indicating the field-induced magnetic transition. The $H_{Cc}$ is 68.5 kOe at 150 K and increases with temperature. Sengupta et al. indicated that the magnetoresistance curves for a polycrystalline $Gd_7Rh_3$ sample show a quadratic variation with external field in the paramagnetic state [8,13]. As shown in the inset of Fig. 3(b), the initial variation of $\Delta\rho/\rho$ with $H$ along *c*-axis of $Gd_7Rh_3$ has the $-H^2$ dependence.

The magnetic field $H$ – temperature $T$ phase diagram along the *c*-axis for $Gd_7Rh_3$ determined from the magnetoresistance and magnetization curves is shown in Fig. 4. As was mentioned above,

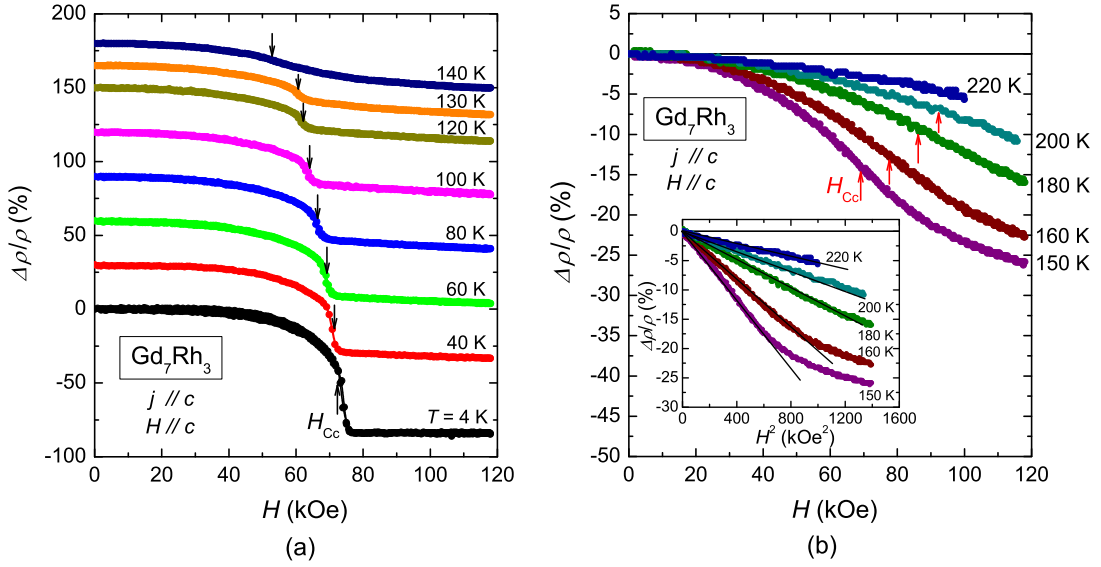


**Fig. 3.** Longitudinal magnetoresistance curves along the *c*-axis ($j$ // $c$ and $H$ // $c$) for a $Gd_7Rh_3$ single crystal at various temperatures. The curves of (a) are plotted with offset in order to make clear the changes with temperature. The inset of (b) indicates the $\Delta\rho/\rho$ vs. $H^2$ curves at 150 K and above.

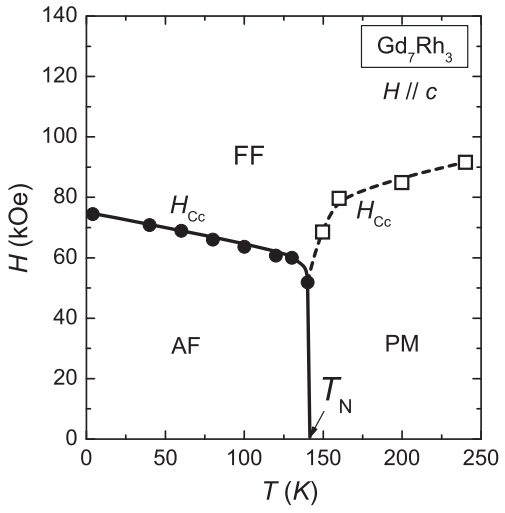


**Fig. 4.** The magnetic field $H$ and temperature $T$ phase diagram for $Gd_7Rh_3$ along the $c$-axis. Solid and dashed lines are guide for the eyes.

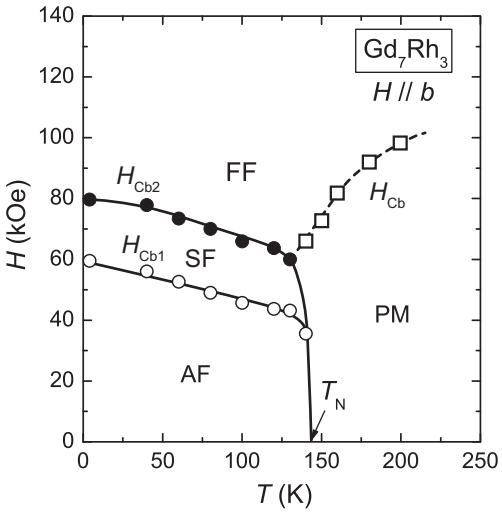


**Fig. 6.** The magnetic field $H$ and temperature $T$ phase diagram for $Gd_7Rh_3$ along the $b$-axis. Solid and dashed lines are guide for the eyes.

the magnetic moments of $Gd^{3+}$ in the AF state may be aligned in the $c$-plane; the external magnetic field, which is applied perpendicular to the magnetic moment, produces the field-induced transition at $H_{Cc}$. The open squares indicate the critical fields of the field-induced transition which is suggested to occur in clusters with short-range AF correlations persisting in a paramagnet matrix. The $H_{Cc}$ above 150 K is larger than that in the AF state.

Transverse magnetoresistance curves ($j$ // $c$ and $H$ // $b$) at various temperatures are shown in Fig. 5. The critical magnetic fields $H_{Cb1}$ and $H_{Cb2}$ along the $b$-axis decrease with increasing temperature up to 140 K. The initial increase of $\Delta\rho/\rho$ disappears at 60 K; the $\Delta\rho/\rho$ becomes almost constant up to $H_{C1}$. The $\Delta\rho/\rho$ value at $H$ = 100 kOe is −28% at 140 K which is the same as that in the longitudinal magnetoresistance. In the paramagnetic state, the magnetoresistance curve indicates the existence of the field-induced transition along the $b$-axis at least up to 200 K; the critical field $H_C$ increases with temperature as well as that in the longitudinal geometry. The quadratic variation of $\Delta\rho/\rho$ with $H$ was observed along the $b$-axis too, as shown in the inset of Fig. 5. Fig. 6 demonstrates the $H$–$T$ phase diagram along the $b$-axis for $Gd_7Rh_3$. Below $T_N$, two successive field-induced magnetic transitions exist from AF to the intermediate spin-flop-like state (SF) and then from SF to the fully saturated FF state. In the paramagnetic state, the single field-induced transition takes place at $H_{Cb}$; the $H_{Cb}$ exceeds 80 kOe above 170 K.

Fig. 7 displays the temperature dependence of the electrical resistivity along the $c$-axis of $Gh_7Rh_3$ with increasing temperature measured without magnetic field as well as the resistivity values obtained from the $\Delta\rho/\rho$ versus $H$ dependences ($H$ // $j$ // $c$) measured at different temperatures (Fig. 3(a)). The $\rho_{FF}$ values correspond to the resistivity in the forced ferromagnetic state just above the critical fields and the $\rho_{100}$ values are the resistivities at $H$ = 100 kOe. By $\rho_{AF}$ we denoted the resistivity measured below $T_N$ at $H$ = 0. The filled area indicates the temperature variation of the difference ($\rho_{AF} - \rho_{FF}$) which is associated with the presence of energy gaps on superzone boundaries below $T_N$. The ($\rho_{AF} - \rho_{FF}$)

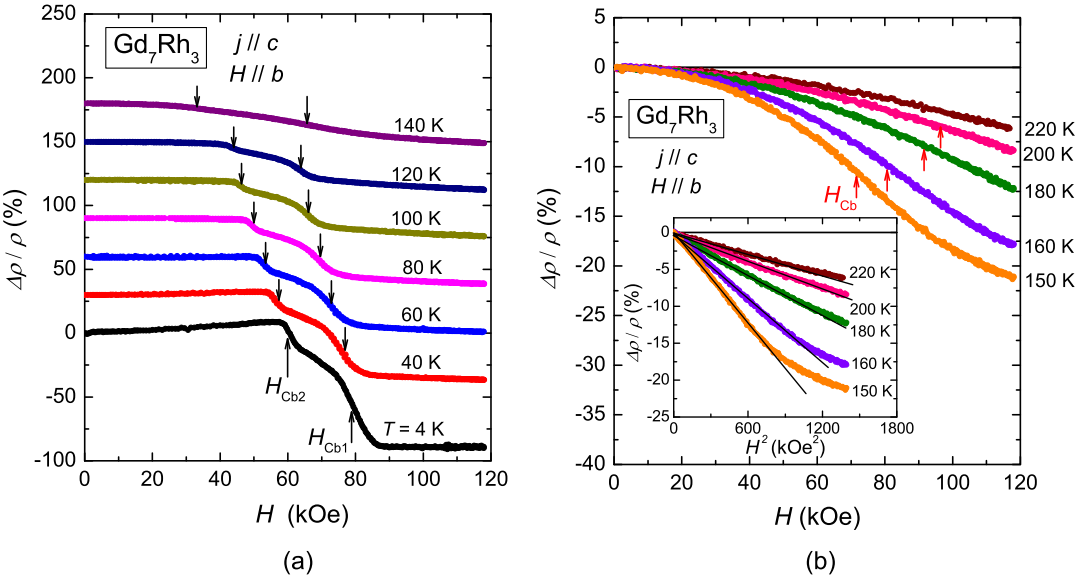


**Fig. 5.** Transverse magnetoresistance curves along the $c$-axis ($j$ // $c$ and $H$ // $b$) for a $Gd_7Rh_3$ single crystal at various temperatures. The curves of (a) are plotted with offset. The inset of (b) indicates the $\Delta\rho/\rho$ vs. $H^2$ curves at 150 K and above.

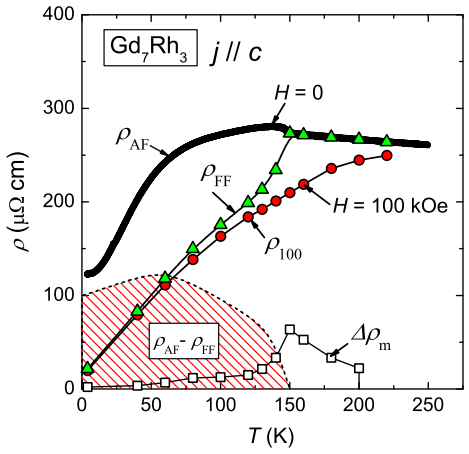


**Fig. 7.** The electrical resistivity for a $Gd_7Rh_3$ single crystal along the *c*-axis as a function of temperature and under external magnetic field derived from the magnetoresistance curves. The $\rho_{FF}$ values correspond to the resistivity in the forced ferromagnetic state just above the critical fields; the $\rho_{100}$ are the resistivity values at $H = 100$ kOe. The filled area indicates the temperature variation of the difference $(\rho_{AF} - \rho_{FF})$. The $\Delta\rho_m(T)$ values obtained as $\Delta\rho_m(T) = \rho(T) - \rho_{100}(T) - \rho_{FF}(T)$.

value demonstrates a non-monotonous change with a maximum around 60 K. It should be noted, that the magnetic susceptibility along the *c*-axis, as was observed in [5], exhibits a non-monotonous behavior as well. Such a correlation may be indicative of changes in the magnetic structure of $Gh_7Rh_3$ with temperature. In Fig. 7, we also plotted the $\Delta\rho_m(T)$ which was obtained by $\Delta\rho_m(T) = \rho(T) - \rho_{100}(T) - \rho_{FF}(T)$ as a function of temperature; the $\rho(T)$ is the total resistivity. Suggesting that the impurity and phonon scattering contributions to the $\rho(T)$ are independent of applied field, the $\Delta\rho_m$ may be associated with the spin disorder and spin fluctuation contributions. As it could be expected, the $\Delta\rho_m(T)$ curve shows a non-monotonous behavior with a maximal value at the magnetic ordering temperature. In an applied field of 100 kOe, the $\Delta\rho_m(T)$ contribution at $T = T_N$ reaches a relatively high value of about 70 μΩ cm. The fact that the zero-field temperature dependence of the resistivity is characterized by a positive $d\rho/dT$ above $T_N$ while the $\rho(T)$ curve measured at 100 kOe has a negative $d\rho/dT$ may be explained by the presence of an additional magnetic contribution to the resistivity caused by short-range antiferromagnetic correlations. The reduction of this contribution with increasing temperature in the paramagnetic region results in a negative value of the temperature coefficient of the resistivity. It is worth to mention that, as in other rare-earth – transition metal intermetallic compounds, the exchange interaction between 4*f* electrons of Gd atoms in $Gd_7Rh_3$ apparently occurs via indirect 4*f*–4*f* coupling [19] through 4*f*–5*d*–4*d*–5*d*–4*f* mechanism and 5*d*–4*d* hybridization. However, short range *f*–*f* correlations alone can hardly be considered as a main reason of unusual behavior of the resistivity in $R_7Rh_3$ above the magnetic ordering temperature. This is because pure rare-earth metals, gadolinium, for instance [20], do not show a negative $d\rho/dT$ in the paramagnetic region despite the presence of short-range spin-correlations up to 800 K [21]. It should be noted, that the absence of a magnetic order in $R_7Rh_3$ compounds with non-magnetic yttrium and lanthanium [4,22] shows that the exchange interaction between 4*d* electrons of rhodium is not strong enough to produce the 4*d*-band splitting. However, the Rh 4*d* electrons in the $R_7Rh_3$ compounds with magnetic rare earth ions may be involved in the exchange interaction, and the *f*–*d* exchange may induce spin fluctuations in the *d*-electron subsystem. These spin fluctuations induced by *f*–*d* exchange are suggested to affect substantially the resistivity behavior in the $R_7Rh_3$-type compounds in analogous to that observed in $R_3T$ ($T$ = Co, Ni, Rh) compounds [23,24]. Further studies are needed in order to examine the role of Rh 4*d* electrons in magnetic and transport properties of $R_7Rh_3$ and answer the question why the short-range AF correlations may persist in these compounds in a wide temperature range above the magnetic ordering temperature.

## 4. Conclusions

As revealed the magnetization measurements in steady and pulsed field, below $T_N = 141$ K, the hexagonal antiferromagnetic compound $Gd_7Rh_3$ shows two successive field-induced magnetic phase transitions in the basal plane and a single transition along the *c*-axis from the initial antiferromagnetic state to the forced ferromagnetic state with parallel alignment of Gd magnetic moments in magnetic fields above 100 kOe. The presence of a small hysteresis in the vicinity of critical fields indicates the first-order nature of the transitions. The field-induced transformations of the magnetic structure in $Gd_7Rh_3$ lead to the giant decrease of the electrical resistivity ($\Delta\rho/\rho \sim 89\%$) which is explained by disappearance of the superzones and energy gaps on the superzone boundaries. The critical field has been determined from *M*–*H* and $\Delta\rho/\rho$–*H* curves; the *H*–*T* phase diagrams for the *b*- and *c*-axes have been constructed. Meanwhile, both the magnetization and magnetoresistance curves above $T_N$ also show inflection points, which are considered as an indication on the field-induced phase transitions in the clusters with antiferromagnetic short-range order persisting in a paramagnetic matrix up to near the room temperature. The negative temperature coefficient of the resistivity observed in $Gd_7Rh_3$ above $T_N$ as well as large magnetoresistance in the paramagnetic state is ascribed to the presence of an additional magnetic contribution to the *s* electron scattering caused by short-range AF correlation. The Rh 4*d* electrons are suggested to be involved in the exchange interactions and affect the transport and magnetic properties of $R_7Rh_3$ compounds.

## Acknowledgments

A part of this work was supported by the program of the Ural Branch of RAS (Project No 12-T-2-1012).

## References

[1] G.L. Olcese, J. Less-Common Met. 33 (1973) 71.
[2] A. Raman, J. Less-Common Met. 26 (1972) 199.
[3] T. Tsutaoka, Y. Nakamori, T. Tokunaga, Y. Itoh, J. Phys. Soc. Jpn. 70 (2001) 199.
[4] O. Loebich, A. Raman, J. Less-Common Met. 43 (1975) 89.
[5] T. Tsutaoka, Y. Nakamori, K. Koyama, T. Tokunaga, J. Magn. Magn. Mater. 293 (2005) 768.
[6] M. Klimczak, E. Talik, R. Troć, K. Gofryk, D. Badurski, J. Alloys Comp. 442 (2007) 172.
[7] E. Talik, M. Klimczak, R. Troć, J. Kusz, W. Hofmeister, A. Damm, J. Alloys Comp. 427 (2007) 30.
[8] K. Sengupta, S. Rayaprol, E.V. Sampathkumaran, Europhys. Lett. 69 (2005) 454.
[9] T. Tsutaoka, D. Noguchi, Y. Nakamori, G. Nakamoto, M. Kurisu, Phys. B 426 (2013) 108.
[10] T. Tsutaoka, Y. Nishiume, T. Tokunaga, Y. Nakamori, Y. Andoh, S. Kawano, G. Nakamoto, M. Kurisu, Phys. B 327 (2003) 352.
[11] T. Tsutaoka, A. Tanaka, Y. Andoh, S. Kawano, M. Kurisu, G. Nakamoto, Phys. B 385 (2006) 353.
[12] K. Sengupta, K.K. Iyer, E.V. Sampathkumaran, Solid State Commun. 139 (2006) 351.
[13] K. Sengupta, S. Rayaprol, E.V. Sampathkumaran, J. Phys.:Condens. Matter 16 (2004) L495.
[14] T. Tsutaoka, K. Shimomura, N.V. Baranov, A.V. Proshkin, E.G. Gerasimov, P.B. Terentev, J. Korean Phys. Soc. 63 (2013) 563.
[15] T. Matsushita, K. Shimomura, T. Tsutaoka, J. Korean Phys. Soc. 63 (2013) 559.
[16] R.J. Elliott, F.A. Wedgwood, Proc. Phys. Soc. London 81 (1963) 846.
[17] N.V. Baranov, P.E. Markin, A.I. Kozlov, E.V. Sinitsyn, J. Alloys Comp. 200 (1993) 43.
[18] N.V. Baranov, A.V. Proshkin, A.F. Gubkin, A. Cervellino, H. Michor, G. Hilscher, E.G. Gerasimov, G. Ehlers, M. Frontzek, A. Podlesnyak, J. Magn. Magn. Mater. 324 (2012) 1907.
[19] I.A. Campbell, J. Phys. F: Met. Phys. 2 (1972) L47.

[20] K. Maezawa, K. Mori, K. Sato, Y. Saito, S. Wakabayshi, J. Phys. Soc. Jpn. 43 (1977) 1815.
[21] J.W. Cable, R.M. Nicklow, Phys. Rev. B 39 (1989) 11732.
[22] Y. Nakamori, H. Fujii, T. Tsutaoka, H. Ito, T. Suzuki, T. Fujita, Phys. B 329–333 (2003) 1087.
[23] N.V. Baranov, G. Hilscher, P.E. Markin, H. Michor, A.A. Yermakov, J. Magn. Magn. Mater. 272–276 (2004) 637.
[24] N.V. Baranov, T. Goto, G. Hilscher, P.E. Markin, H. Michor, N.V. Mushnikov, J-G. Park, A.A. Yermakov, J. Phys.: Condens. Matter 17 (2005) 3445.